Universitat Autònoma de Barcelona

Dipòsit digital de documents de la UAB

This is the **accepted version** of the journal article:

Vélez, Paris; Paredes, Ferran; Casacuberta Orta, Pau; [et al.]. «Portable Reflective-Mode Phase-Variation Microwave Sensor Based on a Rat-Race Coupler Pair and Gain». IEEE sensors journal, Vol. 23, Issue 6 (March 2023), p. 5745-5756. DOI 10.1109/JSEN.2023.3240771

This version is available at https://ddd.uab.cat/record/275092

under the terms of the IN COPYRIGHT license

Portable Reflective-Mode Phase-Variation Microwave Sensor Based on a Rat-Race Coupler Pair and Gain/Phase Detector for Dielectric Characterization

Paris Vélez, *Senior Member, IEEE,* Ferran Paredes, *Senior Member, IEEE,* Pau Casacuberta, *Graduate Student Member, IEEE*, Mahmoud Elgeziry, *Graduate Student Member*, IEEE, Lijuan Su, *Member, IEEE*, Jonathan Muñoz-Enano, *Member, IEEE*, Filippo Costa, *Senior Member, IEEE*, Simone Genovesi, *Senior Member, IEEE*, and Ferran Martín, *Fellow, IEEE*

***Abstract*—This paper presents a low-cost and portable phase-variation planar microwave sensor operating in reflective mode, where the output variable, the phase of the reflection coefficient of the one-port sensing element, is retrieved by means of a distributed circuit based on a pair of rat-race hybrid couplers and the associated electronics. This includes a microcontroller, a voltage controlled oscillator (VCO), a digital-to-analog converter (DAC), and a RF/microwave gain/phase detector. By this means, vector network analyzers (VNAs), i.e., high-cost instruments typically used for obtaining the reflection coefficient in one-port structures, or circulators (microwave components able to separate the injected signal from the reflected signal in any one-port network) are avoided. Indeed, the presented architecture (including the microwave rat-race hybrid configuration and the associated electronics) can be adapted to other one-port reflective-mode phase-variation microwave sensors. A prototype example, where the sensing element is a one-port step-impedance open-ended transmission line, is reported. The device provides the phase of the reflection coefficient of the sensing element as a function of the dielectric constant of the material under test (MUT) with a maximum sensitivity of –65.7º and a relative error of less than 8% in all the measurements.**

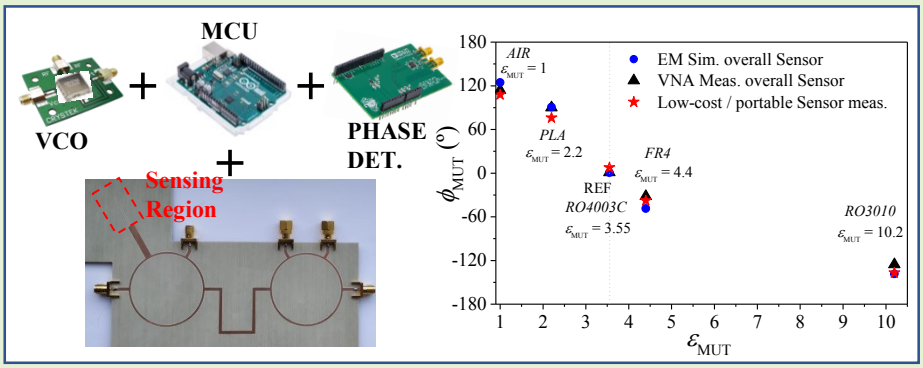

***Index Terms*— Hybrid coupler, microstrip technology, microwave sensor, permittivity sensor, phase detector, phase-variation sensor, reflective-mode sensor.**

I. Introduction

MICROWAVE technologies are well-suited for sensing, and constitute a good alternative to optical sensors (those considered to dominate the sensor's market) in many scenarios [1]. Microwaves are very sensitive to the electromagnetic properties of the media to which they interact. Thus, most microwave sensors, at least those categorized under the designation of non-remote sensors (either contact or contactless), are devices able to provide the dielectric properties of the so-called material under test (MUT), typically the complex permittivity. Nevertheless, there are many other variables related to the permittivity of materials, such as the ambient temperature and humidity, the atmospheric pressure, material composition, etc., Therefore, microwave sensors are useful for the determination of many different physical, chemical, and even biological variables (in some cases, specific functional films, or reagents, are necessary) [1]. The research activity in microwave sensors has been progressively focussed on planar structures, due to their inherent advantages, i.e., low-cost and profile, possibility of sensor implementation in flexible substrates, including polymers [2], organic substrates, such as paper [3], and fabric

This work was supported by MCIN/AEI 10.13039/501100011033, Spain, through the projects PID2019-103904RB-I00 (ERDF European Union) and PDC2021-121085-I00 (European Union Next Generation EU/PRTR), by the AGAUR Research Agency, Catalonia Government, through the project 2017SGR-1159, and by Institució Catalana de Recerca i Estudis Avançats (who awarded Ferran Martín). P. Casacuberta acknowledges the Ministerio de Universidades, Spain, for the FPU grant (Ayudas para la formación de profesorado universitario), ref. FPU20/05700. L. Su acknowledges the Juan de la Cierva Program for the support through the project IJC2019-040786-I.

P. Vélez, F. Paredes, P. Casacuberta, L. Su, J. Muñoz-Enano, and F. Martín are with GEMMA/CIMITEC, Departament d'Enginyeria Electrònica, Universitat Autònoma de Barcelona, 08193 Bellaterra, Spain. (e-mail: Paris.Velez@uab.cat).

M. Elgeziry, F. Costa, and S. Genovesi are with Dipartimento di Ingegneria dell'Informazione, Università di Pisa, 56126 Pisa, Italy.

XXXX-XXXX © XXXX IEEE. Personal use is permitted, but republication/redistribution requires IEEE permission.
See http://www.ieee.org/publications_standards/publications/rights/index.html for more information.

[4], and compatibility with other technologies, e.g., microfluidics [5]-[7], textiles (wearables) [8]-[10], micromachining [11], 3D-printing [12], new materials (e.g., graphene) [13], etc.

Planar microwave sensors can be classified according to various criteria [1]. Some of the categorization schemes are binary, for example, resonant or non-resonant, contact or contactless, transmission or reflective mode, invasive or non-invasive, intrusive or non-intrusive, active or passive, single-ended or differential-mode, etc. However, the most useful classification of planar microwave sensor is the one that obeys to the working principle, or, equivalently, to the considered output variable [1]. Thus, planar microwave sensors can be divided between frequency-variation sensors [14]-[24], phase-variation sensors [25]-[42], frequency-splitting sensors [43]-[51], and coupling-modulation sensors [52]-[66]. Although sometimes differential sensors [27]-[29],[67]-[69] have been included as part of this classification scheme, differential sensing is actually an operational mode, rather than a working principle.

Among the previous categorization of sensors, phase-variation sensors have been the subject of an increasing research interest. The reasons are multiple: (i) such sensors can operate at a single frequency, thereby reducing the costs of the associated electronics in a real scenario (operational environment), (ii) phase measurements are robust against electromagnetic interference (EMI) and noise (similar to frequency measurements); (iii) phase-variation sensors with reduced size and very high sensitivity based on reflective-mode structures (either single-ended or differential) can be implemented (nevertheless, different schemes to boost up the sensitivity in planar microwave sensors based on coupled lines or coupled resonators have been recently reported [70]-[72]). Indeed, reflective-mode phase-variation sensors with unprecedented sensitivities based on either quarter- or half-wavelength open-ended transmission line resonators (the sensing elements) cascaded to high/low impedance inverters have been reported [30] (it has also been demonstrated that by replacing the distributed sensing resonators with semi-lumped resonators, the sensor size can be reduced yet keeping similar performance [36],[37]). More recently, it has been shown that coupled lines [42], or coupled semi-lumped resonators (e.g., step impedance resonators –SIRs) [41], can provide even further sensitivities in reflective-mode phase-variation sensors, by virtue of the strong variation experienced by the phase of the reflection coefficient between the split resonances when the coupling is weak. For example, in one of the devices reported in [30], the sensitivity is as high as 529º (the input variable is the dielectric constant, i.e., dimensionless), whereas in one of the sensors presented in [42], the sensitivity is higher (736º). In both cases, the size of the sensing region is very small.

Despite the significant advantages and high performance (mainly the high sensitivity) of the reflective-mode phase-variation sensors mentioned in the preceding paragraph, retrieving the phase of the reflection coefficient (the output variable) is not absent of certain difficulty, unless vector networks analyzers (VNAs) are used for that purpose (the usual approach in the proof-of-concept demonstrators reported in the available literature). However, VNAs are high-cost components, acceptable for device characterization and measurements at laboratory level, but not in real operational environments. In this paper, we report an approach to retrieve the phase of the reflection coefficient of the sensing element (a one-port reflective mode phase-variation sensor) without the use of VNAs. The injected and the reflected signals from the sensor are separated by means of an arrangement based on hybrid couplers, thereby avoiding the use of circulators (also an expensive component), and the phase is inferred by means of a gain/phase detector. Such VNA-less and circulator-less method to retrieve the phase of the reflection coefficient was first reported in [73]. However, in that work, the gain/phase detector, the key component to infer the output variable of the sensor, was not included. In this work, we include such component and apply the approach to a one-port sensing element based on a high/low step-impedance transmission line configuration terminated with an open-ended distributed resonator. Moreover, additional electronic components, including a voltage controlled oscillator (VCO), a microcontroller, and a digital-to-analog converter (DAC), are introduced in the final fabricated prototype, with the result of a fully portable sensing device that does not need neither a signal generator nor a VNA.

The work is organized as follows. In Section II, the specific circuit schematic (based on a pair of 180º hybrid couplers) for inferring the reflection coefficient of the one-port sensing element from the measurement of the output voltage waves at two different (separated) ports, is presented. Such circuit schematic and the corresponding analysis constituted the main goal of [73], but such analysis is briefly presented in this paper for coherence and completeness. In Section III, the sensing element (a reflective-mode phase-variation sensor based on an open-ended high-impedance quarter-wavelength transmission line resonator cascaded to a low-impedance quarter-wavelength impedance inverter) is presented and analysed. The complete sensor, including the sensing element plus the microwave circuitry necessary to obtain the phase of the reflection coefficient of the sensing element, but excluding the associated electronics, is presented in Section IV. A low-cost and portable reflective-mode phase-variation microwave sensor that includes all the electronics (microcontroller, VCO, DAC, and RF/microwave gain/phase detector) needed for the generation of the feeding signal, as well as for retrieving the output variable, is presented and characterized in Section V. Finally, the main concluding remarks of the work are highlighted in Section VI.

II. Sensor Concept and Circuit Analysis

In two-port transmission-mode sensors the output variable (typically a resonance frequency, a phase, or a magnitude) is contained in the transmission coefficient. Thus, the associated circuitry for retrieving the output variable (without the use of a VNA) consists of a voltage controlled oscillator (VCO) connected to the input port (for the generation of the

interrogation signal of the sensor), plus a phase or envelope detector cascaded to the output port (thereby providing the phase or magnitude, respectively, of the transmission coefficient [74]).

In reflective-mode sensors, the interrogation (injected) signal and the signal containing the relevant information (reflected signal) are present at the same (and unique) port. Therefore, additional components for separating the injected and the reflected signals are needed. Circulators can be used for that purpose, but these elements are expensive. An alternative solution, the one proposed in this paper, and first reported in [73], is based on the use of directional couplers, particularly, 180º rat-race hybrid couplers. Figure 1 depicts the schematic of the whole sensor, including the associated electronics, the sensing element, the pair of rat-race hybrid couplers, and the gain/phase detector, a necessary element to retrieve the phase of the reflection coefficient of the sensing element. Such reflection coefficient is designated as ρ_{MUT} in this work, and the corresponding phase, the output variable of the sensor, as ϕ_{MUT}.

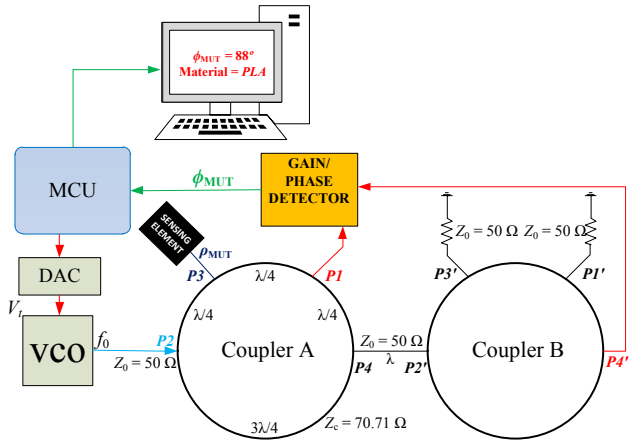

Fig.1. Schematic of the proposed sensor, including the sensing element, connected to port 3 of the left coupler (A), the VCO, connected to port 2 of such coupler, and the gain/phase detector, able to provide the magnitude and phase difference between the signals at ports 1 (left coupler, A) and 4'(right coupler, B). Ports 1' and 3' are terminated with 50-Ω matched loads.

According to the sketch of Fig. 1, the input (harmonic) signal, tuned to the operational frequency of the couplers is injected at the Δ port of coupler A (port 2), whereas the sensing element is connected to port 3 of that coupler. In this work, the frequency of operation f_0 has been set to 2 GHz. Such frequency represents a compromise between the total size of the whole sensor (including the double rat-race configuration and the sensing element) and the simplicity of the associated electronics. The Σ port of coupler A (port 1) is connected to one of the input ports of the gain/phase detector, whereas port 4 is connected to the Δ port of coupler B (port 2') through a 360º line. Note that port designation uses the super-index (') for coupler B, in order to differentiate the ports in that coupler from those of coupler A. Ports 1' and 3' are terminated with matched loads, whereas port 4' is connected to the second input port of the gain/phase detector.

With the considered port designation, the *S*-parameter matrix of the hybrid couplers is [75]

$$\mathbf{S} = \mathbf{S}' = -\frac{j}{\sqrt{2}}\begin{pmatrix} 0 & 0 & 1 & 1 \\ 0 & 0 & 1 & -1 \\ 1 & 1 & 0 & 0 \\ 1 & -1 & 0 & 0 \end{pmatrix} \quad (1)$$

Taking into account the specific port terminations, or loadings, the transmission coefficients between the input port (port 2 of coupler A) and port 1 (of coupler A), and between port 2 and port 4' (of coupler B) can be expressed as [73]

$$S_{12} = \frac{b_1}{a_2} = -\frac{1}{2}\rho_{MUT} \quad (2)$$

$$S_{4'2} = \frac{b_{4'}}{a_2} = -\frac{1}{2} \quad (3)$$

Note that (2) is proportional to the reflection coefficient (ρ_{MUT}) of port 3 of coupler A (where the sensing element is located). The ratio between the output voltage waves at ports 1 (b_1) and 4' ($b_{4'}$), equivalent to the ratio between the transmission coefficients S_{12} (from port 2 to 1) and $S_{4'2}$ (from port 2 to 4'), is thus

$$\frac{b_1}{b_4'} \equiv \frac{S_{12}}{S_{4'2}} = \rho_{\mathrm{MUT}} \quad (4)$$

and it coincides with the reflection coefficient of the sensing element. In [73], where the analysis that leads to expression (4) was discussed in detail, it was demonstrated that the measurement of the transmission coefficients S_{12} and $S_{4'2}$, and application of the ratio given by (2), provides a good estimation of ρ_{MUT}, and particularly of its phase, ϕ_{MUT}. According to (4), ϕ_{MUT} is simply given by the difference between the phases of S_{12} and $S_{4'2}$. Thus, in the present work, the phase ϕ_{MUT} is retrieved by means of a gain/phase detector, a device that gives the phase difference between two signals, as well as the ratio between their magnitudes. For that purpose, the gain/phase detector is arranged as shown in Fig. 1, with the input ports connected to ports 1 and 4' of couplers A and B, respectively.

In order to implement a portable device, avoiding the use of a signal generator, a VCO that provides the feeding (or interrogation) harmonic signal to be injected at port 2 of coupler A is used. The control voltage of the VCO, V_t, is provided by a DAC, in turn managed by a microcontroller (MCU). The microcontroller also receives the output signal of the sensor, from the gain/phase detector, for further data processing and, eventually, storage and visualization (e.g., by means of a computer or a LCD display). Note that in the system of Fig. 1, the control voltage of the VCO, V_t, is a constant value, given by the required operating frequency, f_0. It is independent on the phase retrieved from the gain/phase detector (i.e., the whole structure is not a closed loop system, despite the fact that the MCU has two functions, managing the VCO and processing the sensor data).

III. The Sensing Element, Sensitivity Analysis, and Characterization

The considered sensing element in this paper, connected to port 3 of coupler A, is a reflective-mode phase-variation sensor based on an open-ended high-impedance quarter-wavelength transmission line resonator (the sensitive part, also called sensing line) cascaded to a low-impedance quarter-wavelength impedance inverter (used to boost up the sensitivity, as discussed in [30], and designated by design line). Naturally, such electrical lengths refer to the operational frequency of the sensor, f_0. In [30], a justification (not absent of certain difficulty) of such combination of electrical lengths and characteristic impedances for sensitivity optimization was given. Let us next provide an alternative (and simple) analysis, not published so far, which leads us to the same conclusions in regard to sensitivity optimization. The main hypothesis is that, in order to enhance the sensitivity, it is necessary that the phase of the reflection coefficient, when the sensitive element is loaded with the reference (REF) sample, experiences the maximum possible variation with frequency. If the phase slope is high, the effect of a variation in the dielectric properties of the MUT, in comparison with the REF material, will be an overall shift that is expected to generate a strong variation in the phase at the operating frequency, i.e., a high sensitivity (an aspect illustrated in Fig. 2).

Let us designate by ϕ_s and Z_s the electrical length and characteristic impedance, respectively, of the sensing line, when such line is loaded with the REF material, and let us call the electrical length and characteristic impedance of the design line ϕ and Z, respectively (see Fig. 3). As a first step, let us make the analysis by considering that the sensor is constituted only by the open-ended sensing line (i.e., ϕ = 0º). The impedance seen from the input port of that line is [75]

$$Z_{in} = -jZ_s \cot \phi_s \tag{5}$$

and the corresponding reflection coefficient, referred to Z_0, the reference impedance, is

$$\rho_{REF} = \frac{+Z_0 + jZ_s \cot \phi_s}{-Z_0 + jZ_s \cot \phi_s} \tag{6}$$

Therefore, the phase of the reflection coefficient is

$$\phi_\rho = 2\arctan\left(\frac{Z_s \cot \phi_s}{Z_0}\right) + \pi \tag{7}$$

The derivative of the phase with the angular frequency (phase slope) can be expressed as

$$\frac{d\phi_\rho}{d\omega} = \frac{d\phi_\rho}{d\phi_s}\cdot\frac{d\phi_s}{d\omega} = -\frac{2}{\frac{Z_0}{Z_s}\sin^2\phi_s + \frac{Z_s}{Z_0}\cos^2\phi_s}\cdot\frac{l_s}{v_s} \tag{8}$$

where l_s and v_s are the physical length and phase velocity, respectively, of the sensing line [note that the last term in (8) is easily obtained, since $\phi_s = \omega \cdot l_s/v_s$].

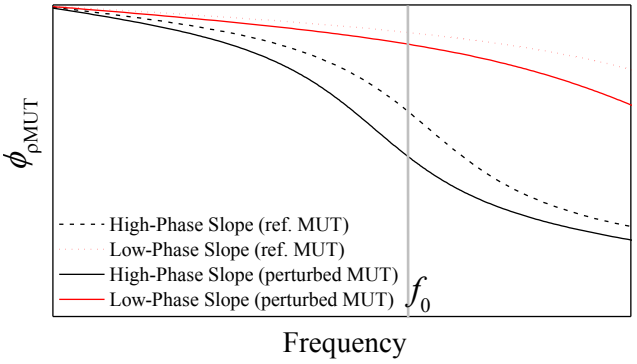

Fig. 2. Sketch illustrating the effects of a high phase slope on the phase variation at a fixed frequency caused by changes in the dielectric constant of the MUT, as compared to a low phase slope.

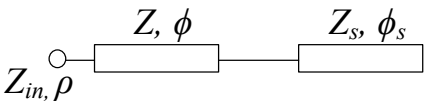

Fig. 3. Schematic of the proposed sensing element with indication of the electrical lengths and characteristic impedances.

In order to obtain the angular frequency, or, equivalently, the electrical length, ϕ_s, that maximizes the phase slope, the second derivative is needed, i.e.,

$$\frac{d^2\phi_\rho}{d\omega^2} = \frac{4\sin\phi_s\cos\phi_s}{\left[\frac{Z_0}{Z_s}\sin^2\phi_s + \frac{Z_s}{Z_0}\cos^2\phi_s\right]^2}\cdot\left\{\frac{Z_0}{Z_s} - \frac{Z_s}{Z_0}\right\}\cdot\frac{l_s^2}{v_s^2} \tag{9}$$

The phase points where the second derivative (9) is null, should correspond to either maxima or minima of the phase slope. The solutions are either $\phi_s = (2n + 1)\cdot\pi/2$, or $\phi_s = n\cdot\pi$, n being an integer. For $\phi_s = (2n + 1)\cdot\pi/2$, the phase slope is

$$\left.\frac{d\phi_\rho}{d\omega}\right|_{\phi_s = (2n+1)\cdot\pi/2} = -\frac{2Z_s}{Z_0}\cdot\frac{l_s}{v_s} \tag{10}$$

corresponding to a maximum, provided $Z_s > Z_0$. For an electrical length satisfying $\phi_s = n\cdot\pi$, the phase slope is

$$\left.\frac{d\phi_\rho}{d\omega}\right|_{\phi_s = n\cdot\pi} = -\frac{2Z_0}{Z_s}\cdot\frac{l_s}{v_s} \tag{11}$$

i.e., a maximum as far as $Z_s < Z_0$.

The main conclusion of the previous analysis is that for optimizing the phase slope, and hence the sensitivity, by using a quarter-wavelength (or odd multiple) sensing line, a high impedance open-ended sensing line is needed. Contrarily, if the sensing element is an open-ended half-wavelength (or multiple) line, the characteristic impedance of such line must be low. Note that such phase and impedance combinations are those corresponding to high-Q resonators. Namely, an open-ended high impedance quarter-wavelength line is equivalent to a high-Q series RLC resonator, whereas an open-ended low impedance half-wavelength line behaves as a high-Q parallel RLC resonator in the vicinity of resonance.

Let us next consider the sensor with the presence of the design line. In this case, the impedance seen from the input port is

$$Z_{in} = \frac{jZ\left(Z\tan\phi - Z_s\cot\phi_s\right)}{Z + Z_s\cot\phi_s\tan\phi} \tag{12}$$

and the reflection coefficient is given by

$$\rho_{REF} = \frac{-Z_0\left(Z + Z_s\tan\phi\cot\phi_s\right) + jZ\left(Z\tan\phi - Z_s\cot\phi_s\right)}{+Z_0\left(Z + Z_s\tan\phi\cot\phi_s\right) + jZ\left(Z\tan\phi - Z_s\cot\phi_s\right)} \tag{13}$$

The phase of the reflection coefficient is thus

$$\phi_\rho = 2\arctan\left(\frac{Z\left(Z_s\cot\phi_s - Z\tan\phi\right)}{Z_0\left(Z + Z_s\tan\phi\cot\phi_s\right)}\right) + \pi \tag{14}$$

Since both ϕ_s and ϕ are frequency dependent, the phase slope in this case can be expressed as follows

$$\frac{d\phi_\rho}{d\omega} = \frac{d\phi_\rho}{d\phi_s}\cdot\frac{d\phi_s}{d\omega} + \frac{d\phi_\rho}{d\phi}\cdot\frac{d\phi}{d\omega} \tag{15}$$

and the derivatives in (15) are:

$$\frac{d\phi_\rho}{d\phi_s} = \frac{-2Z^2Z_sZ_0(1+\tan^2\phi)}{Z_0^2\left(Z\sin\phi_s + Z_s\tan\phi\cos\phi_s\right)^2 + Z^2\left(Z\tan\phi\sin\phi_s - Z_s\cos\phi_s\right)^2} \tag{16a}$$

$$\frac{d\phi_\rho}{d\phi} = \frac{-2ZZ_0\left(Z^2 + Z_s^2\cot^2\phi_s\right)}{Z_0^2\left(Z\cos\phi + Z_s\sin\phi\cot\phi_s\right)^2 + Z^2\left(Z_s\cos\phi\cot\phi_s - Z\sin\phi\right)^2} \tag{16b}$$

$$\frac{d\phi_s}{d\omega} = \frac{l_s}{v_s} \tag{16c}$$

$$\frac{d\phi}{d\omega} = \frac{l}{v} \tag{16d}$$

where l and v are the length and phase velocity of the design line. Since for the structure based merely on the sensing line, the optimum phases are $\phi_s = (2n + 1)\cdot\pi/2$ (with Z_s high), or $\phi_s = n\cdot\pi$ (with Z_s low), i.e., high-Q resonators, as mentioned before, it can be assumed that when a transmission line (design line) is cascaded to the sensing line, the optimum phases of the sensing line are also $\phi_s = (2n + 1)\cdot\pi/2$ (with Z_s high), or $\phi_s = n\cdot\pi$ (with Z_s low). Thus, we should determine the optimum phase and characteristic impedance of the design line.

Let us focus the analysis on the case where the phase of the sensing line is $\phi_s = (2n + 1)\cdot\pi/2$ (since the sensor will be implemented by means of a 90º sensing line). Evaluation of the phase slope [expression (15)] for such phase of the sensing line (leaving ϕ as a free parameter) is

$$\left.\frac{d\phi_\rho}{d\omega}\right|_{\phi_s = (2n+1)\cdot\pi/2} = \frac{-2Z_0}{\left(Z_0^2 + Z^2\tan^2\phi\right)}\cdot\left\{Z_s(1+\tan^2\phi)\cdot\frac{l_s}{v_s} + \frac{Z}{\cos^2\phi}\cdot\frac{l}{v}\right\} \tag{17}$$

and such phase slope is a maximum for those values of ϕ where the derivative of (17) with ϕ nulls. Note that the fact that the phase of the sensing line is set to $\phi_s = (2n + 1)\cdot\pi/2$ determines the operational frequency, provided l_s is set to a certain value. Consequently, we should obtain the derivative of (17) with respect to ϕ, not with respect to the angular frequency. Calculation of such derivative gives

$$\frac{d}{d\phi}\left(\left.\frac{d\phi_\rho}{d\omega}\right|_{\phi_s = (2n+1)\cdot\pi/2}\right) = \frac{-4Z_0\tan\phi\left(Z_0^2 - Z^2\right)}{\cos^2\phi\left(Z_0^2 + Z^2\tan^2\phi\right)^2}\cdot\left\{Z_s\frac{l_s}{v_s} + Z\frac{l}{v}\right\} \tag{18}$$

and it is null for $\phi = (2n + 1)\cdot\pi/2$, or $\phi = n\cdot\pi$. In the former case, the phase slope (17), or (15) with both phases satisfying $\phi_s = \phi = (2n + 1)\cdot\pi/2$, is

$$\left.\frac{d\phi_\rho}{d\omega}\right|_{\phi_s = \phi = (2n+1)\cdot\pi/2} = -\frac{2Z_0}{Z^2}\cdot\left\{Z_s\cdot\frac{l_s}{v_s} + Z\cdot\frac{l}{v}\right\} \tag{19a}$$

whereas for $\phi = n\cdot\pi$ and $\phi_s = (2n + 1)\cdot\pi/2$, the phase slope is

$$\left.\frac{d\phi_\rho}{d\omega}\right|_{\phi_s = \frac{(2n+1)\cdot\pi}{2},\ \phi = n\cdot\pi} = -\frac{2}{Z_0}\cdot\left\{Z_s\cdot\frac{l_s}{v_s} + Z\cdot\frac{l}{v}\right\} \tag{19b}$$

In view of (19), it is apparent that the optimum phase of the design line for enhancement of the phase slope is $\phi = (2n+1)\cdot\pi/2$, provided the characteristic impedance of such line is set to a low value, $Z < Z_0$ [note that Z appears in the denominator of 19(a) squared]. It is also apparent that the characteristic impedance of the sensing line, with $\phi_s = (2n + 1)\cdot\pi/2$ (the considered case), must be set to a high value [see 19(a)].

The previous analysis justifies that the considered sensing element in this paper is based on a pair of cascaded 90º lines with low (the design line) and high (the open-ended sensing line) characteristic impedance. By this means, at the frequency where the phases satisfy such condition, the phase slope (or derivative of the phase of the reflection coefficient with frequency) is expected to be very high, and this enhances the sensitivity in the vicinity of the REF sample. By considering that the input variable of the sensor is the dielectric constant of the MUT, the sensitivity is given by the following expression

$$S = \frac{d\phi_{\mathrm{MUT}}}{d\varepsilon_{\mathrm{MUT}}} \tag{20}$$

where ϕ_{MUT} is the phase of the reflection coefficient at the operating frequency, when it is loaded with a certain MUT sample with dielectric constant $\varepsilon_{\mathrm{MUT}}$. Note that $\phi_{\mathrm{MUT}} = \phi_\rho$ when the MUT coincides with the REF material (or $\varepsilon_{\mathrm{MUT}} = \varepsilon_{\mathrm{REF}}$). A variation of the dielectric constant of the MUT modifies both the electrical length, ϕ_s, and the characteristic impedance, Z_s, of the sensing line. Therefore, the sensitivity can be expressed as

$$S = \frac{d\phi_{MUT}}{d\varepsilon_{MUT}} = \frac{d\phi_{MUT}}{d\phi_s}\cdot\frac{d\phi_s}{d\varepsilon_{MUT}} + \frac{d\phi_{MUT}}{dZ_s}\cdot\frac{dZ_s}{d\varepsilon_{MUT}} \tag{21}$$

However, it can be easily demonstrated [30] that the last term in (21) vanishes for dielectric constants in the vicinity of $\varepsilon_{\mathrm{REF}}$, since $d\phi_{\mathrm{MUT}}/dZ_s = 0$ for $\phi = (2n + 1)\cdot\pi/2$ and $\phi_s = (2n + 1)\cdot\pi/2$. Thus, the sensitivity in the limit of small perturbations around $\varepsilon_{\mathrm{REF}}$ is

$$S_{\varepsilon_{REF}} = \left.\frac{d\phi_{MUT}}{d\varepsilon_{MUT}}\right|_{\varepsilon_{REF}} = \left.\frac{d\phi_{MUT}}{d\phi_s}\cdot\frac{d\phi_s}{d\varepsilon_{MUT}}\right|_{\varepsilon_{REF}} = \left.\frac{d\phi_\rho}{d\phi_s}\cdot\frac{d\phi_s}{d\varepsilon_{MUT}}\right|_{\varepsilon_{REF}} \tag{22}$$

where $d\phi_\rho/d\phi_s\big|_{\varepsilon_{REF}}$ is given by (16a) with $\phi = (2n + 1)\cdot\pi/2$ and $\phi_s = (2n + 1)\cdot\pi/2$, and

$$\left.\frac{d\phi_s}{d\varepsilon_{MUT}}\right|_{\varepsilon_{REF}} = \frac{\omega_0 l_S}{2\sqrt{2}c}\frac{1}{\sqrt{\varepsilon_r\frac{1+F}{(1-F)^2}+\varepsilon_{REF}\frac{1}{1-F}}} \tag{23}$$

where c is the speed of light in vacuum, ε_r is the substrate dielectric constant, and F is a shape factor that depends on the transverse geometry of the line (microstrip technology is considered), i.e.,

$$F = \left(1 + 12\frac{h}{W_s}\right)^{-1/2} \tag{24a}$$

for $W_s/h \geq 1$, or by

$$F = \left(1 + 12\frac{h}{W_s}\right)^{-1/2} + 0.04\left(1 - \frac{W_s}{h}\right)^2 \tag{24b}$$

for $W_s/h < 1$. In (24), h and W_s are the substrate thickness and the width of the sensing line, respectively, and it is assumed that $t << h$, where t is the thickness of the metallic layer. Thus, the sensitivity for $\varepsilon_{MUT} = \varepsilon_{REF}$ is found to be

$$S_{\varepsilon_{REF}} = -2\frac{Z_s Z_0}{Z^2}\cdot\frac{\omega_0 l_s}{2\sqrt{2}c}\frac{1}{\sqrt{\varepsilon_r\frac{1+F}{(1-F)^2}+\varepsilon_{REF}\frac{1}{1-F}}} \tag{25}$$

In the designed sensor, the sensing line has been designed with an electrical length of 90º (corresponding to a quarter-wavelength) at the operating frequency, f_0, and by considering that such line is loaded (covered) with the so-called reference (REF) material, a uniform and semi-infinite material with dielectric constant $\varepsilon_{REF} = 3.55$ (the one of the *Rogers 4003C* low-loss microwave substrate, available in our laboratory). The considered sensor substrate is the *Rogers RO4003C*, with thickness $h = 0.81$ mm, dielectric constant $\varepsilon_r = 3.55$, and loss tangent $\tan\delta = 0.0022$ (note that this is the substrate where the complete sensor will be implemented, to be discussed later). The characteristic impedance of the sensitive high-impedance 90º open-ended line section (sensing line) has been set to $Z_s = 109\ \Omega$, whereas the low-impedance line section (design line) has been designed to exhibit a characteristic impedance of $Z = 30\ \Omega$. With these impedance values and electrical lengths, as well as substrate parameters, the dimensions of the sensing element are those indicated in Fig. 4, where the layout is depicted. Note that the physical length of the high-impedance quarter-wavelength open-ended sensing line is shorter than the one cascaded to it, also a quarter-wavelength line section. The reason is the considered REF material, with $\varepsilon_{REF} = 3.55$, a dielectric constant much higher than that of air ($\varepsilon_{air} = 1$). Moreover, the width of these 90º line sections is unequal.

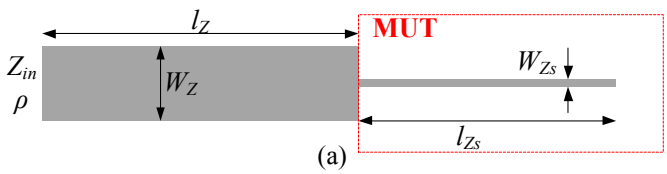

(a)

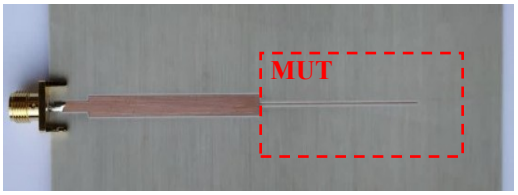

(b)

Fig. 4. Layout of the sensing element and relevant dimensions (a) and photograph of the fabricated structure (b). The sensing region, where the MUT must be located, is shown by the dashed rectangle. Dimensions are (in mm): $l_{Zs} = 19.8$, $W_{Zs} = 0.2$, $l_Z = 21.7$ and $W_Z = 3.8$. Note that the size of the MUT must cover the sensing region, and the MUT should not cover the line adjacent to the sensing region.

The sensor is devoted to the determination of the dielectric constant of the MUT in this work, but it might be applied to the measurement of other variables related to it. Figure 5 depicts the phase of the reflection coefficient at $f_0 = 2$ GHz, ϕ_{MUT}, as a function of the dielectric constant of the MUT, ε_{MUT}, inferred by means of electromagnetic simulation. Such simulations have been performed by means of the *Keysight PathWave Advanced Design System* (ADS) *2021* commercial simulator, and the substrate has been considered semi-infinite in the vertical direction. For $\varepsilon_{MUT} = \varepsilon_{REF} = 3.55$, the phase of the reflection coefficient of the sensing element at f_0 should be $\phi_{MUT} = 0$º, since the open end is translated to the input port of the sensing element due to the presence of two cascaded quarter-wavelength transmission line sections. As it can be seen in Fig. 5, the simulated phase for $\varepsilon_{MUT} = \varepsilon_{REF} = 3.55$ is in good agreement with the expected value (note that the effects of the 50-Ω access lines on the phase have been eliminated). The sensitivity, as defined by (20), is also depicted in Fig. 5. The sensitivity in the limit of small perturbations in the vicinity of the reference dielectric constant, $\varepsilon_{MUT} = \varepsilon_{REF}$, is found to be $S_{sim} = -64.36$º (the sub-index denotes simulated sensitivity), in good agreement with the theoretical value, $S_{th} = -64.53$º, as given by expression (25).

Increasing the sensitivity in the limit of small perturbations (in the vicinity of the dielectric constant of the reference material) has the penalty of losing linearity and input dynamic range. In order to be able to increase the input dynamic range and the sensor linearity, thereby being possible the measurement of dielectric constants beyond the limit considered in this work, it would be enough to relax the condition of maximum sensitivity. For that purpose, the procedure would be to consider the impedances Z and Z_s closer to the reference impedance of the ports, $Z_0 = 50\Omega$. Note that in the limit where only a sensing line with impedance $Z_s = 50\ \Omega$ is considered, the phase variation experienced by the reflection coefficient (ϕ_{MUT}) by varying the dielectric constant of the MUT on top of it should be roughly linear.

To further validate the performance of the sensing element, we have fabricated it by means of the *LPKF H100* drilling machine [see Fig. 4(b)], and we have obtained the phase of the reflection coefficient for different materials (by means of a VNA, model *Agilent PNA N5221A*). The results are also included in Fig. 5, where the good agreement with the simulated phase values can be appreciated (the considered MUTs are stacks of uncladded microwave substrates available in our laboratory, with an enough overall thickness so as to

consider them semi-infinite in the vertical direction). It should be mentioned that the sensitivity as inferred from experimental data cannot be obtained due to the lack of a significant number of data points.

It is worth highlighting that the phase of the reflection coefficient (ϕ_{MUT}) does not vary substantially with the loss tangent of the considered materials, as revealed by electromagnetic simulations (with loss tangents in the range between 0 and 0.1), not shown. The phase dispersion caused by varying loss tangent in the cited range has been found to be less than 2º.

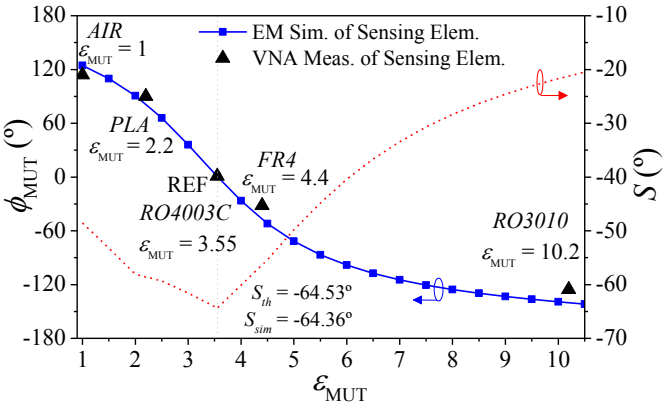

Fig. 5. Dependence of the phase of the reflection coefficient of the sensing element with the dielectric constant of the MUT, and sensitivity.

IV. Complete Sensor and Experimental Validation

As mentioned before, the overall sensor, including the sensing element plus the necessary circuitry for retrieving the phase of the reflection coefficient of the sensing element, ϕ_{MUT}, has been implemented in the same substrate used for the fabrication of the isolated sensing element (see previous section). The rat-race hybrid couplers exhibit a ring circumference of 1.5 wavelengths and a characteristic impedance of Z_c = 70.71 Ω (provided the reference impedance of the ports is Z_0 = 50 Ω, the usual value) [75]. It should be mentioned that the line section of length λ connecting port 4 of coupler A with port 2' of coupler B is not actually necessary. Nevertheless, its presence is convenient in order to physically separate the pair of couplers, thereby avoiding undesired coupling effects (such line does not modify the performance of the sensor since its electrical length at the operating frequency is 360º, equivalent to 0º). With the indicated phase and impedance values, and substrate parameters, the resulting dimensions of the hybrid couplers are those indicated in Fig. 6, where the whole sensor, excluding the associated electronics, is depicted (the sensing element is identical to the one of Fig. 4).

Figure 7 depicts the dependence of the measured phase of the reflection coefficient, ϕ_{MUT}, of the prototype of Fig. 6 as a function of the dielectric constant, ε_{MUT}, of different dielectric samples, previously used in Section III. In order to validate the prototype functionality, the first measurement consisted in determining the phase of the reflection coefficient of the sensing element at f_0 for $\varepsilon_{MUT} = \varepsilon_{REF} = 3.55$, the reference dielectric constant. In order to obtain ϕ_{MUT} = 0º, the phase value corresponding to the dielectric constant of the REF material, it was necessary to slightly shift the operational frequency to f_0 = 2.07 GHz. Such frequency tuning is unavoidable in practice (especially in a multicomponent circuit like the one of Fig. 6) due to fabrication-related tolerances. The measured experimental data (referred to in Fig. 7 as VNA Measurements), obtained with the operating frequency set to f_0 = 2.07 GHz, as indicated, are in good agreement with the simulated phases. Let us clarify that the phase ϕ_{MUT}, the output variable of the sensor, either simulated or measured, has been inferred through the ratio of the transmission coefficients S_{12} and $S_{4'2}$. Such ratio provides the reflection coefficient [see expression (4)], from which the phase can be inferred.

It is important to highlight that the measured data in Fig. 7 is almost undistinguishable from the experimental data in Fig. 5 (inferred by directly measuring the reflection coefficient in the sensing element). This validates the associated microwave circuitry (a pair of 180º rat-race hybrid couplers) to retrieve the phase of the MUT, ϕ_{MUT}, by independent measurements of the phases at ports 1 and 4'. Note that the simulated phases in Figs. 5 and 7 are also undistinguishable. Indeed, the sensitivity (at small perturbations) inferred from the simulated data points of Fig. 7 is found to be S_{sim} = −65.73º, very similar to the value given in Fig. 5, and also in very good agreement with the theoretical value. Notice that a 5-th order polynomial calibration curve with correlation coefficient of R^2 = 0.999 has been included for applications purpose.

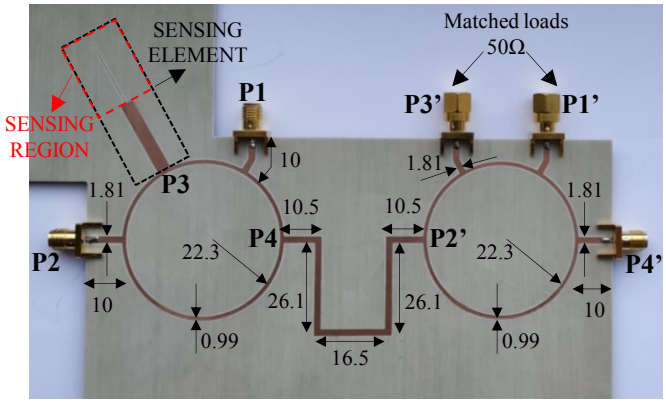

Fig. 6. Photograph of the fabricated sensor including the pair of rat-race couplers. The indicated dimensions are in mm. Note that the dimensions of the sensing element are given in Fig. 4.

Let us also clarify that, concerning the electromagnetic simulations, we have first simulated the whole structure excluding the high-impedance 90º sensing line by means of the *Keysight ADS* electromagnetic solver, and then the sensing line loaded with the different MUT samples. Then the results have been exported to the *Keysight ADS* circuit schematic, which has provided the transmission coefficients S_{12} and $S_{4'2}$, and thereby the phase of interest, ϕ_{MUT}. This co-simulation has been necessary since the MUT only covers the open-ended high-impedance 90º sensing line, and the *Keysight ADS* electromagnetic simulator (a 2D electromagnetic solver) is

unable to deal with such kind of structures, with dielectric layers exhibiting transverse limited boundaries.

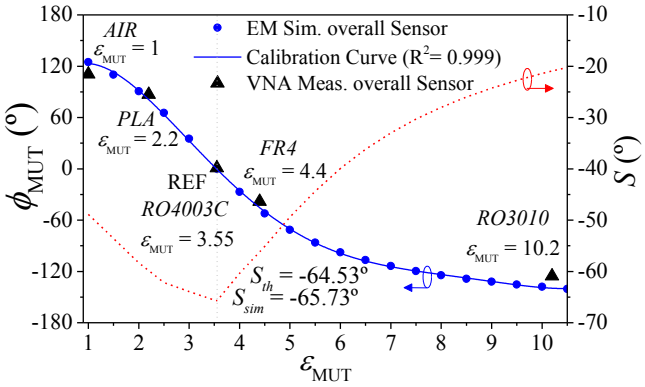

Fig. 7. Dependence of the phase of the reflection coefficient of the sensing element for the sensor of Fig. 4 with the dielectric constant of the MUT, and sensitivity. The calibration curve is $\phi_{MUT} = 82.32 + 97.5\varepsilon_{MUT} - 68.79\varepsilon_{MUT}^2 + 13.18\varepsilon_{MUT}^3 - 1.06\varepsilon_{MUT}^4 + 0.03\varepsilon_{MUT}^5$.

V. LOW-COST AND PORTABLE MICROWAVE SENSOR PROTOTYPE

In the previous section, the sensing data was obtaining by measuring the phases of the transmission coefficients at ports P_1 and $P_{4'}$, as indicated, by means of a VNA (the objective was to validate the functionality of the coupler pair to separate the feeding signal from the signal reflected back from the sensing element). This section is focused on the development of a low-cost portable phase-variation microwave permittivity sensor based on the microwave structure of Fig. 6, and following the sketch of Fig. 1 (thereby avoiding the use of expensive VNA equipment).

Figure 8 shows the photograph of the whole sensor, that includes the electromagnetic block and the required associated electronics (electronic block). The electronic module is in charge of the generation of the feeding signal and post-processing. The feeding microwave harmonic signal (tuned to $f_0 = 2.07$ GHz) is generated by means of a VCO, model *Crystek CVCO55BE*. A DAC, model *Microchip Technologies MCP4725*, connected through the microcontroller (MCU *Arduino*), provides a constant VCO control voltage of $V_t = 3.9$ V. The microcontroller also retrieves the sensor data (provided by the gain-phase detector) and generates the required feeding signals of the different electronic elements (VCO, DAC, and gain-phase detector).

The signals at the two output ports of the microwave sensor (ports P_1 and $P_{4'}$, see Fig. 1 or 6) have been injected to the input ports of a RF/microwave gain/phase detector (model *Analog Devices AD8302*). The gain/phase detector output provides the phase difference of the signals at the input ports, and, consequently, the output variable of the sensor, ϕ_{MUT}. Naturally, such phase can be retrieved for the dielectric constant of the different considered MUTs, and has been processed and monitored externally (in real time) by means of a computer. Figure 9 plots the measured phase shift for the different dielectric materials (the corresponding dielectric constant values are indicated in the figure). For comparison purposes, the simulated and measured phases of Fig. 7, corresponding to the measured dielectric slabs, have been included in the same figure, where it can be seen that the agreement is very reasonable.

In order to evaluate the repeatability and robustness of the whole sensor system, the measurements for each sample were carried out in three different campaings. In the first round of measurements, the samples were tested starting with the lowest dielectric constant MUT, and progressively measuring the phase of those MUTs exhibiting higher dielectric constants (sequence *Air-PLA-RO4003C-FR4-RO3010*). The second round of measurements was done by reversing the MUT sequence (from *RO3010* up to Air). Finally the last round of measurement was done by considering an arbitrary order (*RO4003C-Air-RO3010-FR4* and *PLA*). As it can be seen in Fig. 10, the relative errors obatined for all the experimental data are less than 8%. All the experimental data have been obtained at room temperature (24ºC) conditions, and the dimensions of the dieletric measured slabs are 28 mm × 14mm in all cases.

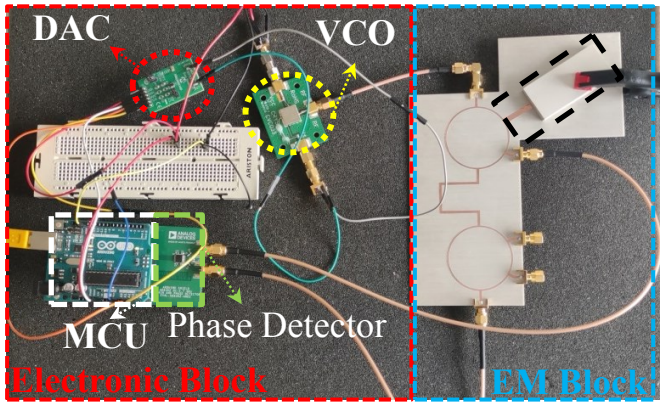

Fig.8. Complete experimental setup of the proposed low-cost and portable reflective-mode phase variation microwave sensor based on a pair of hybrid couplers.

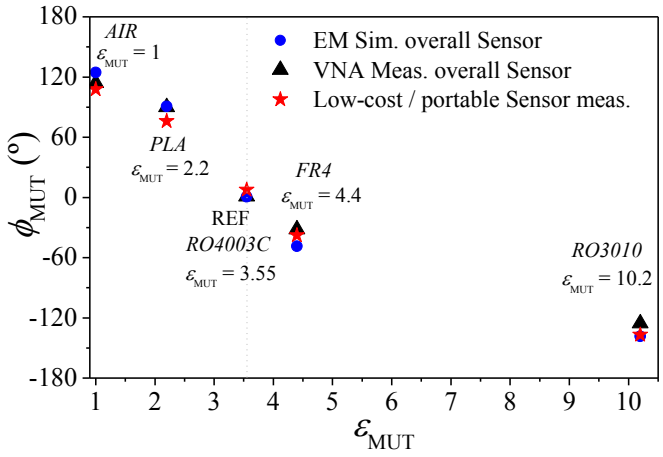

Fig. 9. Dependence of the phase of the reflection coefficient of the sensing element in the portable and low-cost proposed microwave sensor with the dielectric constant of the MUT.

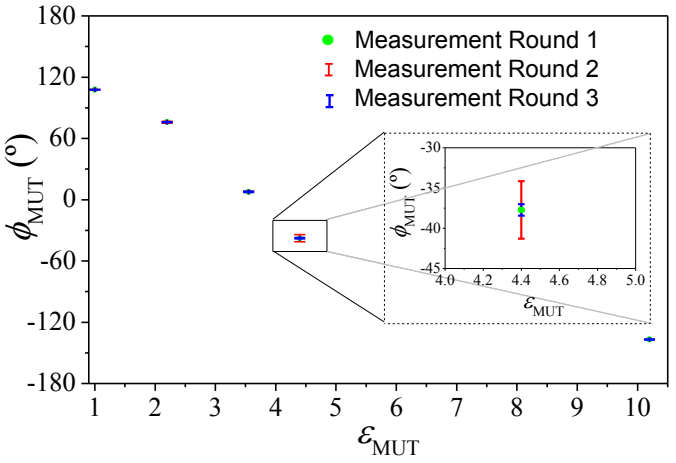

Fig.10. Error bars obtained for the experimental setup of Fig. 6, considering three experimental campaigns.

With the results of Figs. 9 and 10, the portable reflective-mode phase-variation permittivity sensor, based exclusively on an electromagnetic module (the sensing element and the pair of couplers) and the associated electronics (for signal generation and processing), has been experimentally validated. Let us clarify that by "portable" we mean in this work a sensing device which provides the output signal without the need of using neither a VNA, the conventional instrument for demonstrating the functionality of microwave sensors at laboratory level, nor a signal generator, typically used to inject the required interrogation signals. Integrating the different sensor components (microwave circuitry plus electronics) in a compact shield is out of the scope of this paper. Let us also emphasize that the main objective of this work has been to implement and experimentally validate such a fully portable reflective-mode phase-variation sensor, rather than designing and implementing a high performance sensor devoted to a specific application. For that reason, we have validated the sensor by considering the material dielectric constant (of the different MUTs) as the input variable. Nevertheless, many other applications, involving measurands (input variables) able to perturb the phase of the reflection coefficient of the sensing element, not necessarily of the type considered in this paper, can be envisaged, e.g., liquid sensing for industrial processes, bio-sensing, structural health monitoring, material composition determination, etc.

VI. Conclusions

In conclusion, it has been demonstrated in this paper that the phase of the reflection coefficient in one-port networks can be retrieved by means of a gain/phase detector and a pair of rat-race hybrid couplers conveniently connected and loaded. The designed and fabricated structure has been applied to the measurement of the phase of the reflection coefficient in a one-port reflective-mode phase-variation sensor based on an open-ended quarter-wavelength sensing resonator cascaded to a low-impedance quarter-wavelength impedance inverter (used to boost up the sensitivity). The sensor has been first experimentally validated by means of a VNA, considering the sensing element plus the microwave circuitry (based on a pair of rat-race couplers) necessary to separate the feeding signal from the reflected signal from the sensing element. Then, a portable and low-cost VNA-less sensor, that incorporates a gain-phase detector, a VCO, a DAC and a microcontroller (plus the microwave module) has been designed and experimentally validated, by measuring the phase of the reflection coefficient of the sensing element for different dielectric samples (MUTs). It has been verified that the measured phases for the different MUTs, provided by the RF/microwave gain/phase detector, are in good agreement with the expected values (VNA measured). The main contributing aspect of the present paper concerns the fact that it has been demonstrated that the output variable in reflective-mode sensors (the phase of the reflection coefficient in our case) can be obtained without the need of costly VNAs and circulators. The proposed system is able to determine the dielectric constant of low and moderate loss materials with dynamic range between 1 and 10.2 (and loss tangent between 0 and 0.01), showing a maximum sensitivity of –65.7º and error of less than 8%.

References

[1] F. Martín, P. Vélez, J. Muñoz-Enano, L. Su, *Planar Microwave Sensors*, Wiley/IEEE Press, Hoboken, NJ, USA, 2022.

[2] L. Su, X. Huang, W. Guo, and H. Wu, "A Flexible Microwave Sensor Based on Complementary Spiral Resonator for Material Dielectric Characterization," *IEEE Sensors J.*, vol. 20, no. 4, pp. 1893-1903, Feb. 2020.

[3] S. Kim, B. Cook, T. Le, J. Cooper, H. Lee, V. Lakafosis, R. Vyas, R. Moro, M. Bozzi, A. Georgiadis, A. Collado, and M.M. Tentzeris, " Inkjet-printed antennas, sensors and circuits on paper substrate," *IET Microw. Antennas Propag.*, vol. 7, pp. 858-868, 2013.

[4] P. Vélez, F. Martín, R. Fernández-García, and I. Gil, "Embroidered Textile Frequency-Splitting Sensor based on Stepped-Impedance Resonators", *IEEE Sensors J.*, vol. 22, no. 9, pp. 8596-8603, May 2022.

[5] K. Grenier *et al.*, "Integrated Broadband Microwave and Microfluidic Sensor Dedicated to Bioengineering," *IEEE Trans. Microw. Theory Techn.*, vol. 57, no. 12, pp. 3246-3253, Dec. 2009.

[6] A. Salim and S. Lim, "Review of Recent Metamaterial Microfluidic Sensors" *Sensors*, vol. 18, no. 1, paper 232, 2018.

[7] M.H. Zarifi, H. Sadabadi, S.H, Hejazi, *et al.*, "Noncontact and Nonintrusive Microwave-Microfluidic Flow Sensor for Energy and Biomedical Engineering," *Sci. Rep.*, vol. 8, paper 139, 2018.

[8] V. Cioffi, A. Raffo and S. Costanzo, "Preliminary Validations of Textile Wearable Microwave Sensor for Biomedical Applications," *2019 13th Europ. Conf. Ant. Propag.* (EuCAP), 2019, pp. 1-2.

[9] M. Martínez-Estrada, I. Gil, and R. Fernández-García, "An alternative method to develop embroidery textile strain sensors," *Textiles*, vol. 1, no. 3, pp. 504–512, Nov. 2021.

[10] X. Lin, Y. Chen, Z. Gong, B. -C. Seet, L. Huang and Y. Lu, "Ultrawideband Textile Antenna for Wearable Microwave Medical Imaging Applications," *IEEE Trans. Ant. Propag.*, vol. 68, no. 6, pp. 4238-4249, Jun. 2020.

[11] G. Lammel *et al.*, "Next generation pressure sensors in surface micromachining technology," *The 13th International Conference on Solid-State Sensors, Actuators and Microsystems*, 2005. Digest of Technical Papers. TRANSDUCERS '05., 2005, pp. 35-36, Vol. 1.

[12] B. D. Wiltshire and M. H. Zarifi, "3-D Printing Microfluidic Channels With Embedded Planar Microwave Resonators for RFID and Liquid Detection," *IEEE Microw.Wireless Compon. Lett.*, vol. 29, no. 1, pp. 65-67, Jan. 2019.

[13] A. Javadian-Saraf, E. Hosseini, B. D. Wiltshire, M. H. Zarifi, M. Arjmand, "Graphene oxide/polyaniline-based microwave split-ring resonator: A versatile platform towards ammonia sensing, *Journal of Hazardous Materials*, vol. 418, paper 126283, 2021.

[14] M. Puentes, C. Weiß, M. Schüßler, and R. Jakoby, "Sensor array based on split ring resonators for analysis of organic tissues," in *IEEE MTT-S Int. Microw. Symp.*, Baltimore, MD, USA, Jun. 2011, pp. 1−4.

[15] M. Schüßler, C. Mandel, M. Puentes, and R. Jakoby, "Metamaterial inspired microwave sensors," *IEEE Microw. Mag.*, vol. 13, no. 2, pp. 57–68, Mar. 2012.

[16] M. S. Boybay and O. M. Ramahi, "Material characterization using complementary split-ring resonators," *IEEE Trans. Instrum. Meas*., vol. 61, no. 11, pp. 3039−3046, Nov. 2012.

[17] C.-S. Lee and C.-L. Yang, "Complementary split-ring resonators for measuring dielectric constants and loss tangents," *IEEE Microw. Wireless Compon. Lett.*, vol. 24, no. 8, pp. 563−565, Aug. 2014.

[18] C.-L. Yang, C.-S. Lee, K.-W. Chen, and K.-Z. Chen, "Noncontact measurement of complex permittivity and thickness by using planar resonators," *IEEE Trans. Microw. Theory Techn.*, vol. 64, no.1, pp. 247−257, Jan. 2016.

[19] L. Su, J. Mata-Contreras, P. Vélez, F. Martín, "Estimation of the complex permittivity of liquids by means of complementary split ring resonator (CSRR) loaded transmission lines", *2017 IEEE MTT-S International Microwave Workshop Series on Advanced Materials and Processes* (IMWS-AMP 2017), Pavia, Italy, 20-22 Sep. 2017.

[20] L. Su, J. Mata-Contreras, P. Vélez, B. Fernández-Prieto and F. Martín, "Analytical method to estimate the complex permittivity of oil Samples", *Sensors*, 18(4), paper 984, 2018.

[21] B.K, Jha, N, Delmonte, A, Lamecki, M, Mrozowski, M, Bozzi, "Design of microwave-based angular displacement sensor", *IEEE Microw. Wireless Compon. Lett.*, vol. 29 (4), pp. 306-308, Apr. 2019.

[22] J. Muñoz-Enano, P. Vélez, M. Gil, F. Martín, "Frequency variation sensors for permittivity measurements based on dumbbell-shaped defect ground structures (DB-DGS): analytical method and sensitivity analysis", *IEEE Sensors J.*, vol. 22, no. 10, pp. 9378-9386, May 2022.

[23] M. Abdolrazzaghi and M. Daneshmand, "A 4 GHz Near-Field Monitoring Planar Oscillator Sensor", *IEEE MTT-S International Microwave Workshop Series on Advanced Materials and Processes for RF and THz Applications (IMWS-AMP)*, Ann Arbor, MI, USA, 2018, pp. 1-3.

[24] M. Abdolrazzaghi, V. Nayyeri, and F. Martín, "Techniques to Improve the Performance of Planar Microwave Sensors: A review and Recent developments", *Sensors*, 22 (18), paper 6946, 2022.

[25] C. Damm, M. Schussler, M. Puentes, H. Maune, M. Maasch and R. Jakoby, "Artificial transmission lines for high sensitive microwave sensors," *IEEE Sensors Conf.,* Christchurch, New Zealand, pp.755−758, Oct. 2009.

[26] F.J. Ferrández-Pastor, J.M. García-Chamizo and M. Nieto-Hidalgo, "Electromagnetic differential measuring method: application in microstrip sensors developing", Sensors, vol. 17, p. 1650, 2017.

[27] J. Muñoz-Enano, P. Vélez, M. Gil, F. Martín, "An analytical method to implement high sensitivity transmission line differential sensors for dielectric constant measurements", *IEEE Sensors J.*, vol. 20, pp. 178-184, Jan. 2020.

[28] M. Gil, P. Vélez, F. Aznar, J. Muñoz-Enano, and F. Martín, "Differential sensor based on electro-inductive wave (EIW) transmission lines for dielectric constant measurements and defect detection", *IEEE Trans. Ant. Propag*., vol. 68, pp. 1876-1886, Mar. 2020.

[29] J. Muñoz-Enano, P. Vélez, M. Gil, J. Mata-Contreras, and F. Martín, "Differential-mode to common-mode conversion detector based on rat-race couplers: analysis and application to microwave sensors and comparators", *IEEE Trans. Microw. Theory Techn*., vol. 68, pp. 1312-1325, Apr. 2020.

[30] J. Muñoz-Enano, P. Vélez, L. Su, M. Gil, P. Casacuberta, and F. Martín, "On the sensitivity of reflective-mode phase variation sensors based on open-ended stepped-impedance transmission lines: theoretical analysis and experimental validation", *IEEE Trans. Microw. Theory Techn*. vol. 69, no. 1, pp. 308-324, Jan. 2021.

[31] L. Su, J. Muñoz-Enano, P. Velez, P. Casacuberta, M. Gil and F. Martin, "Highly Sensitive Phase Variation Sensors Based on Step-Impedance Coplanar Waveguide (CPW) Transmission Lines," *IEEE Sensors J*., vol. 21, no. 3, pp. 2864-2872, Feb. 2021.

[32] P. Casacuberta, J. Muñoz-Enano, P. Vélez, L. Su, M. Gil, and F. Martín, "Highly sensitive reflective-mode detectors and dielectric constant sensors based on open-ended stepped-impedance transmission lines", *Sensors*, vol. 20, paper 6236, 2020.

[33] J. Coromina, J. Muñoz-Enano, P. Vélez, A. Ebrahimi, J. Scott, K. Ghorbani, F. Martín, "Capacitively-Loaded Slow-Wave Transmission Lines for Sensitivity Improvement in Phase-Variation Permittivity Sensors", *50th Europ. Microw. Conf*., Utrecht, The Netherlands Sep. 2020.

[34] A. Ebrahimi, J. Coromina, J. Muñoz-Enano, P. Vélez, J. Scott, K. Ghorbani, and F. Martín, "Highly Sensitive Phase-Variation Dielectric Constant Sensor Based on a Capacitively-Loaded Slow-Wave Transmission Line," *IEEE Trans. Circ. Syst. I: Reg. Papers*, vol. 68, no. 7, pp. 2787-2799, Jul. 2021.

[35] L. Su, J. Muñoz-Enano, P. Vélez, P. Casacuberta, M. Gil, F. Martín, "Phase-Variation Microwave Sensor for Permittivity Measurements Based on a High-Impedance Half-Wavelength Transmission Line," *IEEE Sensors J*., vol. 21, no. 9, pp. 10647-10656, May 2021.

[36] L. Su, J. Muñoz-Enano, P. Vélez, M. Gil, P. Casacuberta, and F. Martín, "Highly sensitive reflective-mode phase-variation permittivity sensor based on a coplanar waveguide (CPW) terminated with an open complementary split ring resonator (OCSRR)," *IEEE Access*, vol. 9, pp. 27928-27944, 2021.

[37] P. Casacuberta, P. Vélez, J. Muñoz-Enano, L. Su, M. Gil, A. Ebrahimi and F. Martín, "Circuit analysis of a Coplanar waveguide (CPW) terminated with a step-impedance resonator (SIR) for highly sensitive one-port permittivity sensing," *IEEE Access*, vol. 10, pp. 62597-62612, 2022.

[38] A. K. Jha, A. Lamecki, M. Mrozowski, and M. Bozzi, "A highly sensitive planar microwave sensor for detecting direction and angle of rotation," *IEEE Trans. Microw. Theory Techn*., vol. 68, no. 4, pp. 1598–1609, Apr. 2020

[39] A. K. Horestani, Z. Shaterian and F. Martín, "Rotation Sensor Based on the Cross-Polarized Excitation of Split Ring Resonators (SRRs)", *IEEE Sensors J*., vol 20, pp. 9706-9714, Sep. 2020.

[40] J. Muñoz-Enano, P. Vélez, L. Su, M. Gil, and F. Martín, "A reflective-mode phase-variation displacement sensor", *IEEE Access*, vol. 8, pp. 189565-189575, Oct. 2020.

[41] P. Casacuberta, P. Vélez, J. Muñoz-Enano, L. Su, M. Gil-Barba and F. Martín, "Reflective-Mode Phase-Variation Permittivity Sensors Based on Coupled Resonators", *IEEE Sensors 2022*, Dallas, Texas, USA, Oct. 30 - Nov. 2, 2022.

[42] P. Casacuberta, P. Vélez, J. Muñoz-Enano, L. Su, and F. Martín "Highly sensitive reflective-mode phase-variation permittivity sensors using coupled line sections", *IEEE Trans. Microw. Theory Techn*., accepted.

[43] B. K. Horestani, J. Naqui, Z. Shaterian, D. Abbott, C. Fumeaux, and F. Martín, "Two-dimensional alignment and displacement sensor based on movable broadside-coupled split ring resonators," *Sensors and Actuators A*, vol. 210, pp. 18–24, Apr. 2014.

[44] J. Naqui, *et al*., "Transmission lines loaded with pairs of magnetically coupled stepped impedance resonators (SIRs): modeling and application to microwave sensors," *IEEE MTT-S Int. Microwave Symp*., Tampa, FL, USA, Jun. 2014, pp. 1–4.

[45] L. Su, J. Naqui, J. Mata-Contreras, and F. Martín "Modeling metamaterial transmission lines loaded with pairs of coupled split ring resonators," *IEEE Ant. Wireless Propag. Lett.*, vol. 14, pp. 68–71, 2015.

[46] L. Su, J. Naqui, J. Mata-Contreras, and F. Martín, "Modeling and applications of metamaterial transmission lines loaded with pairs of coupled complementary split ring resonators (CSRRs)," *IEEE Ant. Wireless Propag. Lett.*, vol. 15, pp. 154–157, 2016.

[47] J. Naqui, C. Damm, A. Wiens, R. Jakoby, L. Su, J. Mata-Contreras, and F. Martín, "Transmission Lines Loaded with Pairs of Stepped Impedance Resonators: Modeling and Application to Differential Permittivity Measurements", *IEEE Trans. Microw. Theory Techn*., vol. 64, no. 11, pp. 3864-3877, Nov. 2016.

[48] L. Su, J. Mata-Contreras, J. Naqui, and F. Martín, "Splitter/combiner microstrip sections loaded with pairs of complementary split ring resonators (CSRRs): modeling and optimization for differential sensing applications," *IEEE Trans. Microw. Theory Techn*., vol. 64, pp. 4362-4370, Dec. 2016.

[49] P. Vélez, L. Su, K. Grenier, J. Mata-Contreras, D. Dubuc, and F. Martín, "Microwave microfluidic sensor based on a microstrip splitter/combiner configuration and split ring resonators (SRR) for dielectric characterization of liquids", *IEEE Sensors J.*, vol. 17, pp. 6589-6598, Oct. 2017.

[50] A. Ebrahimi, J. Scott, and K. Ghorbani, "Differential sensors using microstrip lines loaded with two split-ring resonators," *IEEE Sens. J*., vol. 18, pp. 5786-5793, 2018.

[51] A. Ebrahimi, G. Beziuk, J. Scott, and K. Ghorbani, "Microwave differential frequency splitting sensor using magnetic-LC resonators," *Sensors*, vol. 20, p. 1066, 2020.

[52] J. Naqui, M. Durán-Sindreu and F. Martín, "Novel sensors based on the symmetry properties of split ring resonators (SRRs)," *Sensors*, vol 11, pp. 7545−7553, 2011.
[53] J. Naqui, M. Durán-Sindreu, and F. Martín, "Alignment and position sensors based on split ring resonators," *Sensors*, vol. 12, pp. 11790−11797, 2012.
[54] B.K. Horestani, C. Fumeaux, S.F. Al-Sarawi, and D. Abbott, "Displacement sensor based on diamond-shaped tapered split ring resonator," *IEEE Sens. J.*, vol. 13, pp. 1153–1160, 2013.
[55] J. Naqui and F. Martín, "Angular displacement and velocity sensors based on electric-LC (ELC) loaded microstrip lines," *IEEE Sensors J.*, vol. 14, no. 4, pp. 939–940, Apr. 2014.
[56] B.K. Horestani, J. Naqui, D. Abbott, C. Fumeaux, and F. Martín, "Two-dimensional displacement and alignment sensor based on reflection coefficients of open microstrip lines loaded with split ring resonators," *Elec. Lett.*, vol. 50, pp. 620–622, Apr. 2014.
[57] B. Ebrahimi, W. Withayachumnankul, S. F. Al-Sarawi and D. Abbott, "Metamaterial-Inspired Rotation Sensor With Wide Dynamic Range," *IEEE Sensors J.*, vol. 14, no. 8, pp. 2609-2614, Aug. 2014.
[58] J. Naqui, J. Coromina, B. Karami-Horestani, C. Fumeaux, and F. Martín, "Angular displacement and velocity sensors based on coplanar waveguides (CPWs) loaded with S-shaped split ring resonator (S-SRR)," *Sensors*, vol. 15, pp. 9628–9650, 2015.
[59] C. Herrojo, F. Paredes, and F. Martín, "Double-stub loaded microstrip line reader for very high data density microwave encoders", *IEEE Trans. Microw. Theory Techn.*, vol.67(9), pp. 3527-3536, Sep. 2019.
[60] C. Herrojo, F. Paredes, and F. Martín, "3D-printed high data-density electromagnetic encoders based on permittivity contrast for motion control and chipless-RFID", *IEEE Trans. Microw. Theory Techn*., vol. 68, no. 5, pp. 1839-1850, May 2020.
[61] C. Herrojo, F. Paredes, and F. Martín "3D-printed all-dielectric electromagnetic encoders with synchronous reading for measuring displacements and velocities", *Sensors*, vol. 20, p. 4837, 2020.
[62] F. Paredes, C. Herrojo, F. Martín, "Microwave Encoders with Synchronous Reading and Direction Detection for Motion Control Applications", *2020 IEEE-MTT-S Int. Microw. Symp.* (IMS'20), Los Angeles, CA, USA, 21-26 Jun., 2020.
[63] C. Herrojo, F. Paredes, and F. Martín "Synchronism and Direction Detection in High-Resolution/High-Density Electromagnetic Encoders", *IEEE Sensors J.*, vol. 21, no. 3, pp. 2873-2882, Feb. 2021.
[64] F. Paredes, C. Herrojo, F. Martín, "Position sensors for industrial applications based on electromagnetic encoders", *Sensors*, vol. 21, pp. 2738 (28 pages), 2021.
[65] F. Paredes, C. Herrojo, F. Martín, "3D-printed quasi-absolute electromagnètic encoders for chipless-RFID and motion control applications", *Electronics*, vol. 10, paper 1154, 2021.
[66] F. Paredes, C. Herrojo, A. Moya, M. Berenguel-Alonso, D. Gonzalez, J. Bruguera, C. Delgado-Simao, and F. Martín, "Electromagnetic Encoders Screen-Printed on Rubber Belts for Absolute Measurement of Position and Velocity", *Sensors*, vol. 22, paper 2044, 2022.
[67] P. Vélez, K. Grenier, J. Mata-Contreras, D. Dubuc, and F. Martín, "Highly-Sensitive Microwave Sensors Based on Open Complementary Split Ring Resonators (OCSRRs) for Dielectric Characterization and Solute Concentration Measurement in Liquids," *IEEE Access*, vol. 6, pp. 48 324–48 338, 2018.
[68] P. Vélez, J. Muñoz-Enano, K. Grenier, J. Mata-Contreras, D. Dubuc, and F. Martín, "Split Ring Resonator-Based Microwave Fluidic Sensors for Electrolyte Concentration Measurements," *IEEE Sensors J.*, vol. 19, no. 7, pp. 2562–2569, Apr. 2019.
[69] P. Vélez, J. Muñoz-Enano, M. Gil, J. Mata-Contreras, and F. Martín, "Differential Microfluidic Sensors Based on Dumbbell-Shaped Defect Ground Structures in Microstrip Technology: Analysis, Optimization, and Applications," *Sensors*, vol. 19, no. 14, p. 3189, Jan. 2019.
[70] A. M. Albishi, M. K. E. Badawe, V. Nayyeri, and O. M. Ramahi, "Enhancing the Sensitivity of Dielectric Sensors With Multiple Coupled Complementary Split-Ring Resonators," *IEEE Trans. Microw. Theory Tech.*, vol. 68, no. 10, pp. 4340–4347, Oct. 2020.
[71] J. Sorocki, I. Piekarz, K. Wincza, S. Gruszczynski, and J. Papapolymerou, "Broadband Microwave Microfluidic Coupled-Line Sensor With 3-D-Printed Channel for Industrial Applications," *IEEE Trans. Microw. Theory Tech*., vol. 68, no. 7, pp. 2808–2822, Jul. 2020.
[72] Z. R. Omam, V. Nayyeri, S.-H. Javid-Hosseini, and O. M. Ramahi, "Simple and High-Sensitivity Dielectric Constant Measurement Usinga High-Directivity Microstrip Coupled-Line Directional Coupler," *IEEE Trans. Microw. Theory Tech*., pp. 1–10, 2022.
[73] M. Elgeziry, F. Paredes, P. Vélez, F. Costa, S. Genovesi, F. Martín, "A Method to Retrieve the Output Variables in Reflective-Mode Phase-Variation Sensors", 52nd Europ. Microw. Conf., Milan, Italy, 20-25 Sep. 2022.
[74] P. Vélez, J. Muñoz-Enano, A. Ebrahimi, C. Herrojo, F. Paredes, J. Scott, K. Ghorbani, and F. Martín, "Single-Frequency Amplitude-Modulation Sensor for Dielectric Characterization of Solids and Microfluidics", *IEEE Sensors J.*, vol. 21, no. 10, pp. 12189-12201, May 2021.
[75] D. M. Pozar, *Microwave Engineering*, 4th Ed., John Wiley, Hoboken, NJ, USA, 2011.

Paris Vélez (S'10-M'14-SM'21) was born in Barcelona, Spain, in 1982. He received the degree in telecommunications engineering, specializing in electronics, the degree in electronics engineering, and the PhD degree in electrical engineering from the Universitat Autònoma de Barcelona, Spain, in 2008, 2010, and 2014, respectively. His PhD thesis concerned common-mode suppressed differential microwave circuits based on metamaterial concepts and semi-lumped resonators. During the PhD degree, the Spanish Government awarded him a Pre-Doctoral Teaching and Research Fellowship from 2011 to 2014. From 2015 to 2017, he was involved in subjects related to metamaterial-based sensors for fluidic detection and characterization at LAAS-CNRS through a TECNIOSpring Fellowship cofounded by the Marie Curie Program. From 2018 to 2020, he has worked in the miniaturization and optimization of passive RF/microwave circuits and sensors based on metamaterials through the Juan de la Cierva Fellowship. He is nowadays Postdoctoral Researcher in CIMITEC, Universitat Autonoma de Barcelona, Spain. His current research interests include the optimization and miniaturization of planar sensors, microfluidic sensors and textile-based sensors. He is a Reviewer for the IEEE TRANSACTIONS ON MICROWAVE THEORY AND TECHNIQUES and many other journals.

Ferran Paredes (M'14-SM'22) received the Telecommunications Engineering degree from the Universitat Autònoma de Barcelona in 2006 and the PhD degree in Electronics Engineering from the same university in 2012. He is working as a Research Assistant at the Universitat Autònoma de Barcelona and his research interests include metamaterial concepts, passive microwaves devices, antennas, and RFID.

Pau Casacuberta (GS'22) was born in Sabadell (Barcelona), Spain, in 1997. He received the Bachelor's Degree in Electronic Telecommunications Engineering and Computer Engineering from the Universitat Autònoma de Barcelona (UAB) in 2020, and the master's degree in Telecommunications Engineering in 2022. He received the Collaboration fellowship by the Spanish Government in 2019 for developing his Bachelor's Thesis in highly sensitive microwave sensors based in stepped impedance structures. Furthermore, he is currently working in the elaboration of his PhD, which is focused on the development of microwave sensors for the characterization of the composition of multicomponent liquid substances, with a research grant from FPU Program of the Universities Spanish Ministry.

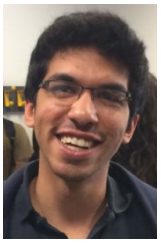

Mahmoud Elgeziry (GS'21) received the B.Sc in mechanical engineering from the British University in Egypt, Cairo, Egypt in 2015 and the M.Sc degree in mechanical engineering from the Polytechnic University of Milan, Milan, Italy, in 2018. He is currently pursuing his Ph.D. degree in the department of Information Engineering at the University of Pisa, Italy. His current research interests include the design of Radio frequency and microwave sensors.

Lijuan Su (S'14-M'18) was born in Qianjiang, Hubei, China in 1983. She received the B.S. degree in communication engineering and the M.S. degree in circuits and systems from the Wuhan University of Technology, Wuhan, China, in 2005 and 2013, respectively, and the Ph.D. degree in electronic engineering from the Universitat Autonoma de Barcelona, Barcelona, Spain, in 2017. From Nov. 2017 to Dec. 2019, she worked as a Postdoctoral Researcher with the Flexible Electronics Research Center, Huazhong University of Science and Technology, Wuhan, China. She is currently a Postdoctoral Researcher under the support of the Juan de la Cierva Program in CIMITEC, Universitat Autonoma de Barcelona, Spain. Her current research interests focus on the development of novel microwave sensors with improved performance for biosensors, dielectric characterization of solids and liquids, defect detection, industrial processes, and so on.

Jonathan Muñoz-Enano was born in Mollet del Vallès (Barcelona), Spain, in 1994. He received the Bachelor's Degree in Electronic Telecommunications Engineering in 2016 and the Master's Degree in Telecommunications Engineering in 2018, both at the Universitat Autònoma de Barcelona (UAB), Spain. In July 2022, he obtained the PhD degree within the doctoral program in Electronics Engineering and Telecommunication in the same university, with the Thesis entitled "Highly Sensitive Planar Microwave Sensors for dielectric characterization of solids, liquids, and biosamples". Actually, he is working as a Postdoctoral Research in CIMITEC, Universitat Autònoma de Barcelona, Spain.

Filippo Costa (S'07–M'11–SM'19) received the M.Sc. degree in telecommunication engineering and the Ph.D. degree in applied electromagnetism from the University of Pisa, Pisa, Italy, in 2006 and 2010, respectively. In 2009, he was a Visiting Researcher with the Department of Radio Science and Engineering, Aalto University, Espoo, Finland. From 2015 to 2017, he was a Short-Term Visiting Researcher with the Grenoble Institute of Technology, Valance, France, and University Rovira I Virgili, Tarragona, Spain. He is currently with the University of Pisa. His current research interests include metamaterials, metasurfaces, antennas, and radio frequency identification. He was selected among the outstanding reviewers of the IEEE TRANSACTIONS ON ANTENNAS AND PROPAGATION (2015-2021) and the IEEE ANTENNAS AND WIRELESS PROPAGATION LETTERS (2017,2018). He was recipient of the Young Scientist Award of the URSI International Symposium on Electromagnetic Theory, URSI General Assembly and URSI AT-RASC in 2013, 2014 and 2015, respectively. Dr. Costa serves as an Associate Editor for IEEE TRANSACTIONS ON ANTENNAS AND PROPAGATION, IEEE ANTENNAS AND WIRELESS PROPAGATION LETTERS, IEEE SENSORS LETTERS, Sensors and Electronics.

Simone Genovesi (S'99-M'07-SM'19) received the Laurea degree in telecommunication engineering and the Ph.D. degree in information engineering from the University of Pisa, Pisa, Italy, in 2003 and 2007, respectively. Since 2003 he has been collaborating with the Electromagnetic Communication Laboratory, Pennsylvania State University (Penn State), University Park. From 2004 to 2006 he has been a research associate at the ISTI institute of the National Research Council of Italy (ISTI-CNR) in Pisa. During the period 2015-2017, he was several times a short-term Visiting Researcher at Grenoble Institute of Technology, Valence, France and at University Rovira I Virgili, Tarragona, Spain. He is currently an Associate Professor at "Dipartimento di Ingegneria dell'Informazione", University of Pisa. Simone Genovesi is the Coordinator of the Additive Manufacturing founded in the framework of the Departments of Excellence ("Dipartimenti di Eccellenza") funded by the Italian Ministry of Education, University and Research. He is an Associate Editor of the IEEE Transactions on Antennas and Propagation. Current research topics focus on additive manufacturing, sensors, radio frequency identification (RFID) systems, reconfigurable antennas.

Ferran Martín (M'04-SM'08-F'12) was born in Barakaldo (Vizcaya), Spain in 1965. He received the B.S. Degree in Physics from the Universitat Autònoma de Barcelona (UAB) in 1988 and the PhD degree in 1992. From 1994 up to 2006 he was Associate Professor in Electronics at the Departament d'Enginyeria Electrònica (Universitat Autònoma de Barcelona), and since 2007 he is Full Professor of Electronics. In recent years, he has been involved in different research activities including modelling and simulation of electron devices for high frequency applications, millimeter wave and THz generation systems, and the application of electromagnetic bandgaps to microwave and millimeter wave circuits. He is now very active in the field of metamaterials and their application to the miniaturization and optimization of microwave circuits and antennas. Other topics of interest include microwave sensors and RFID systems, with special emphasis on the development of high data capacity chipless-RFID tags. He is the head of the Microwave Engineering, Metamaterials and Antennas Group (GEMMA Group) at UAB, and director of CIMITEC, a research Center on Metamaterials supported by TECNIO (Generalitat de Catalunya). He has organized several international events related to metamaterials and related topics, including Workshops at the IEEE International Microwave Symposium (years 2005 and 2007) and European Microwave Conference (2009, 2015 and 2017), and the Fifth International Congress on Advanced Electromagnetic Materials in Microwaves and Optics (Metamaterials 2011), where he acted as Chair of the Local Organizing Committee. He has acted as Guest Editor for six Special Issues on metamaterials and sensors in five International Journals. He has authored and co-authored over 650 technical conference, letter, journal papers and book chapters, he is co-author of the book on Metamaterials entitled *Metamaterials with Negative Parameters: Theory, Design and Microwave Applications* (John Wiley & Sons Inc.), author of the book *Artificial Transmission Lines for RF and Microwave Applications* (John Wiley & Sons Inc.), co-editor of the book *Balanced Microwave Filters* (Wiley/IEEE Press), co-author of the book *Time-Domain Signature Barcodes for Chipless-RFID and Sensing Applications* (Springer), and co-author of the book *Planar Microwave Sensors* (Wiley/IEEE Press). Ferran Martín has generated 22 PhDs, has filed several patents on metamaterials and has headed several Development Contracts.

Prof. Martín is a member of the IEEE Microwave Theory and Techniques Society (IEEE MTT-S). He is reviewer of the IEEE Transactions on Microwave Theory and Techniques and IEEE Microwave and Wireless Components Letters, among many other journals, and he serves as member of the Editorial Board of IET Microwaves, Antennas and Propagation, International Journal of RF and Microwave Computer-Aided Engineering, and Sensors. He is also a member of the Technical Committees of the European Microwave Conference (EuMC) and International Congress on Advanced Electromagnetic Materials in Microwaves and Optics (Metamaterials). Among his distinctions, Ferran Martín has received the 2006 Duran Farell Prize for Technological Research, he holds the *Parc de Recerca UAB – Santander* Technology Transfer Chair, and he has been the recipient of three ICREA ACADEMIA Awards (calls 2008, 2013 and 2018). He is Fellow of the IEEE and Fellow of the IET.